JMEPEG (2007) 16:554–558
DOI: 10.1007/s11665-007-9089-0

1059-9495/$19.00

Investigation of In situ Cu-TiB$_2$ Composite on the Copper Using Laser Melting Synthesis

L.Y. Gu, G.Y. Liang, and Z.B. Zheng

(Submitted March 24, 2006; in revised form October 16, 2006)

A surface composite layer reinforced with TiB$_2$ particles was produced on copper by use of the laser remelting in situ synthesis. The microstructure, electrical conductivity, and sliding wear behavior of the in situ Cu-TiB$_2$ composite were investigated. The experimental results show that the size of reinforcing TiB$_2$ particles is about 800 nm and the microhardness of composite layer reaches HV 210. Although the electrical conductivity of the composite layer is reduced with increasing TiB$_2$ volume fraction, the decrease of the integrated conductivity of the samples containing composite layer and copper substrate is insignificant. The wear resistance of composite layer is 10 times better than that of the copper sample.

Keywords composite, copper, laser remelting, TiB$_2$

1. Introduction

The particle reinforced copper alloys have been developed because of their high strength and good conductivity, especially at elevated temperature (Ref 1-3). High-strength/high-conductivity Cu alloys can be achieved by reinforcing or dispersing ceramic particles, such as oxides (Ref 4), borides (Ref 5), carbides (Ref 6), and nitrides (Ref 7) in the Cu matrix. The TiB$_2$ particles, among others, are potential candidates for reinforcement of Cu alloy, because of their high-melting point, hardness, and thermal conductivity. Recently, an in situ technique was developed to fabricate TiB$_2$ particle-reinforced metal matrix composites (MMCs) (Ref 8, 9). The basic principle of this technique is that the fine and thermodynamically stable ceramic phases are in situ formed by the exothermic reaction between elements and compound within a metal matrix. The in situ composites exhibited improved mechanical strength, enhanced wear resistance, and remained electrically conductive (Ref 10). However, the establishment of high strength and high hardness is dependent on sacrificing conductivity due to the limitation of reinforced particle volume fraction.

High-strength copper alloys exhibit good wear resistance and temperature resistance as well as high-electric conductivity in many cases. In the case of composites, conductivity of the bulk composite is limited due to the amount of the second phase ceramic particles. If the composite layer only forms on the surface of copper alloys, it is possible that the loss of the conductivity can be reduced to the smallest lever when the wear resistance is improved.

High-power laser has been used to improve the mechanical and chemical behavior of metallic materials surface. It has been successfully applied to improve wear resistance and corrosion resistance of ferrous alloys, aluminum alloys, and other nonferrous alloys (Ref 11-16). However, whether the TiB$_2$ composite can be in situ synthesized during very short laser scanning time has not been reported.

The present study deals with the coating of Cu-Ti-B$_4$C powder mixture that was remelted using a laser, and an in situ Cu-TiB$_2$ composite layer was created on the copper. The microstructure, electrical conductivity, and wear resistance of the composite layer were investigated.

2. Experimental Procedure

Cu powder (99.5% purity), Ti powder (99.5% purity), and B$_4$C powder (90%) with an average size of 75, 100, and 75 μm, respectively, were used as coating materials. Using B$_4$C is because of economic reason and low Gibbs free energy of formation of TiB$_2$, which is near to that of elements B and Ti. Four standard powder mixtures were prepared by milling Cu, Ti, and B$_4$C powders for 2 h in a high-energy ball mill filled with argon gas. During ball milling, the mass ratio of ball to powder mixture was 20:1. The target composition of powder mixtures is to form the different volume fractions of TiB$_2$, that is 5, 8, 14, and 20 vol.% TiB$_2$ in copper matrix after laser melting in situ synthesis. The composition of powders used in this investigation is shown in Table 1.

The substrate was the electrical copper plate, which was machined to 50 × 24 × 6 mm^3 size. Before the laser scanning, the powder mixture was predeposited on the sample's surface by bonding. The bonding agent was nitrocellulose diluted by acetone. Laser melting in situ synthesis was conducted using a 5 kW continuous transverse flow CO$_2$ laser. After laser technology was optimized, the laser process parameters were selected as follows: laser power was 3.2 kW; laser beam diameter was 1.5 mm; scanning speed was 7.5 mm/s, and the overlapping interval was 0.5 mm. Helium gas was used as shielding gas to prevent oxidation of

L.Y. Gu, Department of Materials Engineering, Xian Institute of Technology, Xian 710032, P.R. China; **G.Y. Liang** and **Z.B. Zheng,** Department of Materials Physics, Science School, Xi'an Jiaotong University, Xi'an 710049, P.R. China. Contact e-mail: gyliang@mail.xjtu.edu.cn.

Table 1 Chemical composition of powder mixtures and volume fraction of TiB_2 in composite layer

	Chemical composition, wt.%				
Sample no.	**Cu**	**Ti**	**B_4C**	**Expected volume fraction of TiB_2, vol.%**	**Actual volume fraction of TiB_2, vol.%**
CM1	72	14	14	20	20.46
CM2	88	6	6	14	13.14
CM3	94	3	3	8	9.34
CM4	96	2	2	5	5.10

the samples. Under the optimum laser parameters, not only the predeposited powder layer with little substrate copper can be completely melted, but also the good coating quality can be achieved. The thickness of predeposited power was 0.6 mm, and that of the in situ composite layer was about 0.25 mm after laser remelting.

After laser remelting, the vertical section of sample was taken perpendicular to the laser scanning trace, and the microstructure was observed. A foil about 0.2 mm thick was cut from the laser melted composite layer. After reducing the foil to less than 0.1 mm thickness, the TEM film specimen was made by electropolishing using a twin jet polisher. Observation and analysis of the microstructure were performed on an S-2700 scanning electron microscope (SEM) and a JEM-200CX transmission electron microscope (TEM). X-ray diffraction analysis was carried out on Rigaku D/max-rA X-ray analyzer (CuK_α).

The microhardness was measured using a Vickers hardness tester with a diamond pyramid indentor at a load of 50 g. The electrical conductivity of samples was measured using a typical four-probe method with help of HP 34401 multimeter (accuracy 0.1 $\mu\Omega$). The samples for electrical conductivity were cut from the top of laser synthesized composite layer and raw sample with the size $50 \times 5 \times 0.5$ mm^3. In order to measure the integrated electrical conductivity of surface composite layer and substrate, 6 mm thick plates containing the laser surface composite layer and substrate copper were adopted. The TiB_2 volume fraction in the laser melted composite layer was measured using the image analysis method on a computer. The volume fraction is an average value of more than 10 areas measured using a scanning electron microscope.

The sliding wear test was carried out using a block-on-ring apparatus (Fig. 1) under the condition of oil lubrication. The upper sample is a block with the laser melted composite layer that was used as wear surface. The sample was machined to a size of $12 \times 3 \times 6$ mm^3. The lower sample was a ring of low-carbon steel containing 0.2% C, with a hardness of HB 80. It was 40 mm in outer diameter and 10 mm in width, with a surface roughness of $R_a = 0.8\,\mu$m. The lubricant was 10# machine oil and it was dropped at the rate of one drop per 15 s. A normal load of 100 N was used. The rotational speed of the ring was 200 rev/min and the total wear distance was 5000 m. The weight loss of the block was measured in an analytical balance of 0.0001 g precision. The weight loss was converted to volume loss values.

3. Experimental Results

3.1 Microstructure of the Laser Melted In situ Composite

Figure 2 shows an image of the Cu-TiB_2 in situ composite from vertical section of sample CM2 (containing 14 vol.% TiB_2 particles). It clearly shows that the composite layer, the substrate, and the interface.

Two vertical sectional SEM images of the laser melted composite layer of samples CM1 and CM3 are shown in Fig. 3. It is seen that there are a lot of ceramic particles in the composite layer. The average size of these ceramic particles is about 800 nm. The x-ray analysis revealed (Fig. 4) that these ceramic particles are TiB_2.

Two x-ray diffraction patterns are shown in Fig. 4, one is that of the raw Cu-Ti-B_4C powder mixture milled for 2 h (Fig. 4a) and the other is that of laser melted in situ composite of sample CM1. It is seen that after laser remelting, the raw

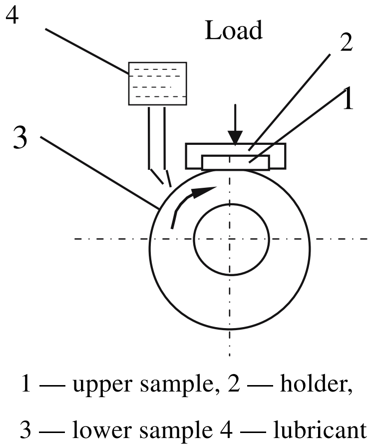

Fig. 1 Schematic illustration of the block-on-ring apparatus

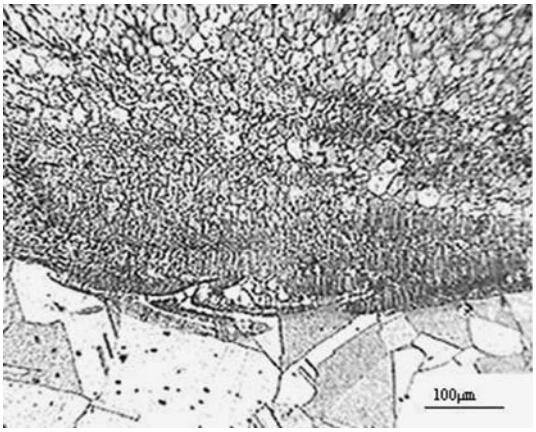

Fig. 2 Optical micrograph of composite layer and substrate of sample CM2

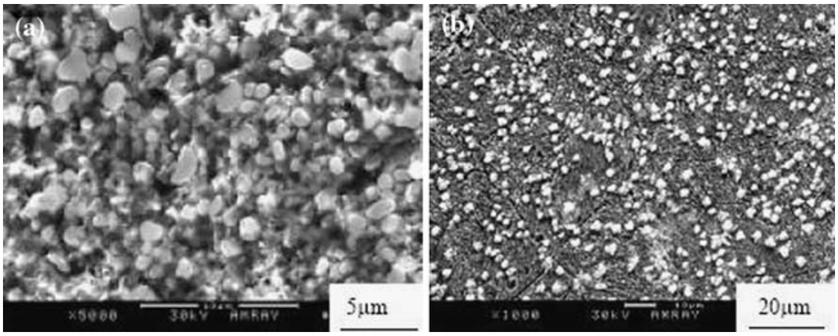

Fig. 3 SEM images of composite layer on the vertical section of sample CM1 (a) and CM3 (b)

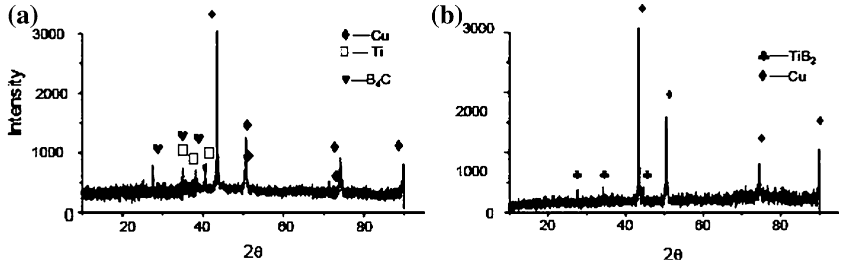

Fig. 4 X-ray diffraction patterns of original powder and laser melted sample CM1 (a) Cu-Ti-B_4C powder mixture (b) laser melted in situ composite of CM1 (20 vol.% TiB_2)

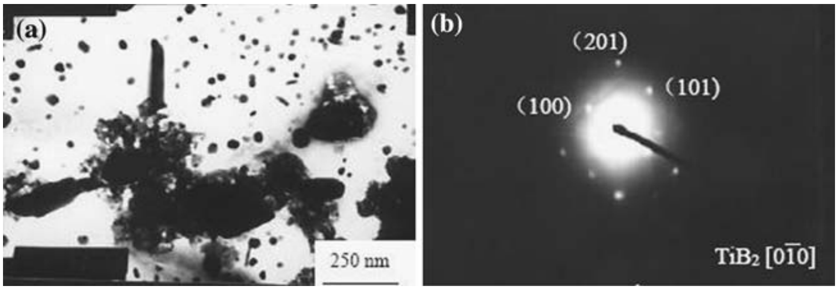

Fig. 5 TEM bright field image (a) electron diffraction pattern (b) of the laser melted in situ composite layer of CM1

powder is fully transformed into TiB_2 and forms a Cu-TiB_2 surface composite layer. Similar x-ray patterns were also exhibited in other samples containing different volume fractions of TiB_2.

TEM bright field image and its electron diffraction pattern of laser melted in situ composite layer of sample CM1 are shown in Fig. 5. From TEM bright field image, it is seen that besides large ceramic particles, some nanometer size particles exist in the laser melted composite layer. Indexing confirmed that these are TiB_2 particles (Fig. 5b).

3.2 The Electrical Conductivity of the Laser Melted In situ Composite

A comparison of the expected volume fraction and measured volume fraction of TiB_2 in the laser melted in situ composite is shown in Table 1. It is seen that the measured volume fraction of TiB_2 basically agrees with the expected value.

Figure 6 displays the relationship of the electrical conductivity and the volume fraction of TiB_2. The electrical conductivity (IACS) is defined as 100% when the electrical resistivity of annealed pure copper is $0.017241\,\Omega\,\mathrm{mm}^2/\mathrm{m}$. In Fig. 5, curve 1 shows the conductivity of the laser melted in situ composite layers and curve 2 shows the integrated conductivity

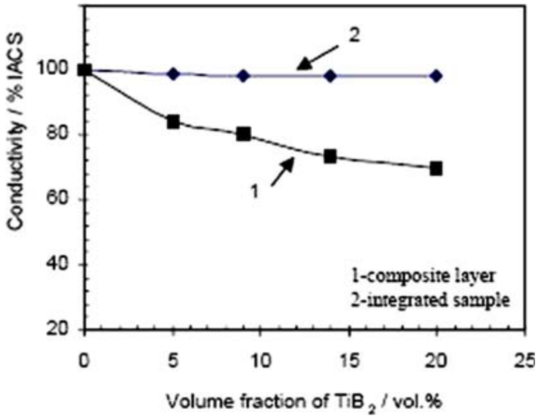

Fig. 6 The relationship of electrical conductivity and TiB_2 volume fraction

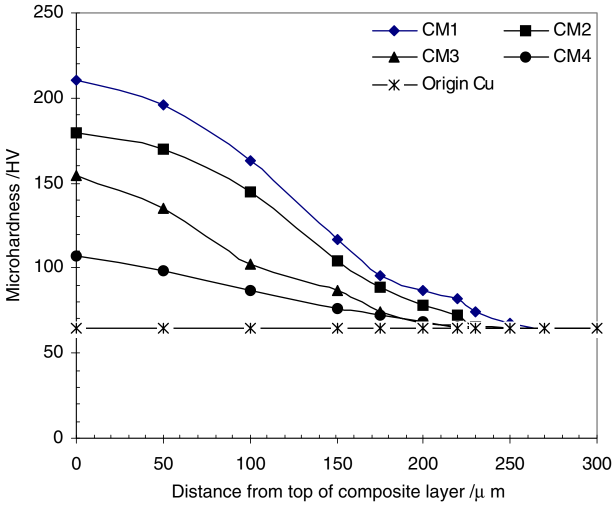

Fig. 7 The variation of microhardness as a function of distance from the top of composite layer

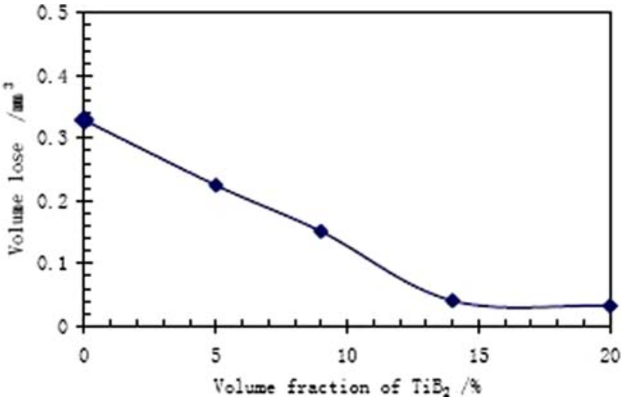

Fig. 8 Volume loss of composites with different volume fraction of TiB_2

of the laser melted in situ composite layer containing different TiB_2 contents and copper substrate. From curve 1, it is seen that the electrical conductivity gradually reduces with increasing volume percent of TiB_2 in the composite layer. When the volume fraction of TiB_2 is increased to 20%, the conductivity (IACS) reaches about 70% IACS. It is also seen that in spite of a decrease in the electrical conductivity of the laser melted in situ composite layer, the integrated electrical conductivity with composite layer and substrate decreases very slightly. For example, the conductivity of the sample CM1 can reach 98% IACS.

3.3 Microhardness and Wears Resistance of the Laser Melted In situ Composite Layer

The variation of microhardness as a function of the distance from the top surface of in situ composite layer is shown in Fig. 7. It is seen that the microhardness increases with increasing volume fraction of TiB_2. The highest hardness (HV210) was obtained in sample CM1 (containing 20 vol.% TiB_2), which is three times as large as raw copper sample.

A comparison of the wear volume loss of composites with different volume fractions of TiB_2 is shown in Fig. 8. It can be seen that TiB_2 is quite effective to improve the wear resistance of copper. When the TiB_2 volume fraction increases to 20 vol.%, the wear volume of composite is only 0.032 mm^3, and the wear resistance is 10 times better than the raw copper sample. It is also seen that the improvement of the wear resistance is very obvious when the volume fraction of TiB_2 is increased to 14 vol.%.

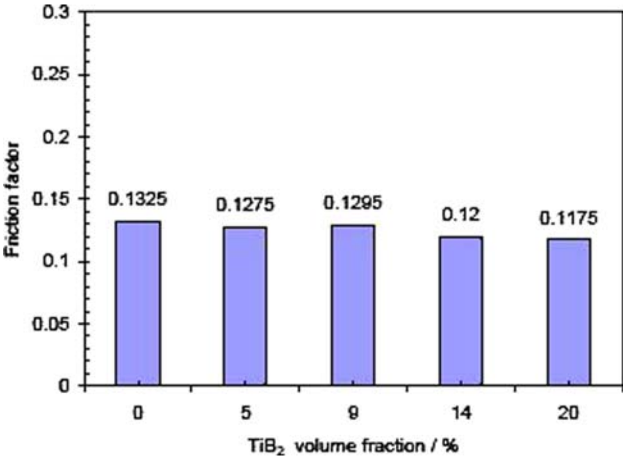

Fig. 9 Variation of the friction factor with TiB_2 volume fraction

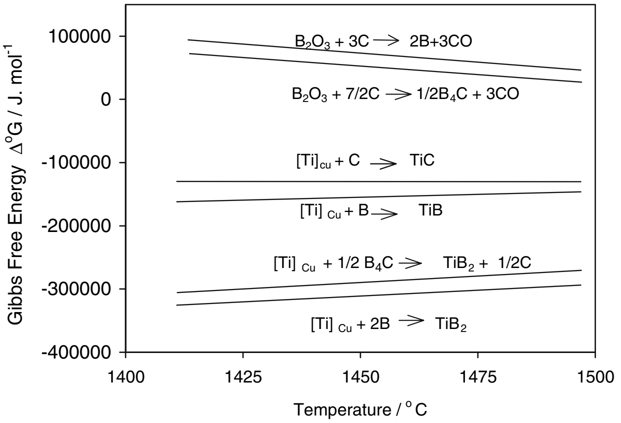

Fig. 10 Plot of ΔG° against temperature for the reactions in Cu-Ti-B melt

The variation of the friction factor with TiB_2 volume fraction is shown in Fig. 9. It is seen that the friction factors of the composite layer with different TiB_2 contents are similar to one another. The friction factors of all samples are found to be in the range of 0.115-0.13. The friction factor of composite layer is slightly smaller than that of the copper sample.

4. Discussion

Under the high heat flux of laser melting, the B_4C would dissolve, and the B-C-Ti system exists in the Cu melt. In the B-C-Ti system, some chemical reactions take place in the molten liquid Cu alloy. The thermodynamic data for the reactions between 1400 and 1500 °C are plotted in Fig. 10 (Ref 8).

Due to its higher thermodynamic stability, TiB_2 phase is likely produced in the laser melted coating. Element carbon used as a deoxidant can reduce the oxidation of boron and copper during laser melting. On the other hand, a few TiC particles could form when the titanium is abundant. According to the x-ray analysis (Fig. 4b), no evidence of TiC was found in the composite layer, which suggests that the quantity of TiC is very little. As the shape and behavior of TiC phase are similar to those of TiB_2, the effect of TiC alone is insignificant.

Referring to Fig. 4(b), it is found that no evidence of residual titanium and B_4C exists in the composite layer. Under the higher heat flux of laser melting, the reaction rate of TiB_2 synthesis is quite fast, which makes the TiB_2 synthesis complete. This suggests that the surface composite of Cu-TiB_2 can be produced if the energy of laser scanning is high enough.

The TiB_2 particles residing in the copper matrix scatter the conductive electrons so that the electrical conductivity of copper matrix composite was reduced. On the other hand, as no coupled structure occurs between TiB_2 particles and copper matrix, the dislocation density in the copper matrix increases insignificantly. It makes the in-situ TiB_2 composite retain higher conductivity because the dislocations also scatters conductive electrons.

Meanwhile, the integrated electrical resistance of the composite layer and substrate copper can be simplified as a parallel and series circuit of the composites resistance and copper substrate resistance. As the thickness of copper is much larger than that of the composite layer, the effect on conductivity of TiB_2 in the composite layer is quite small.

As TiB_2 particles possess very high hardness, they protrude from the wear surface in sliding wear. This causes the hard phases TiB_2 in the copper matrix to support larger load and the soft copper matrix to reserve oil. This constitution can help to reduce friction and improve wear resistance under lubricated sliding wear condition. With increasing TiB_2 volume fraction, the hardness of composite increases and the wear resistance improves. As friction factor mainly depends on the load and speed under oil lubrication condition, the effect of the material character is reduced. Meanwhile, the constitution of hard TiB_2 particles and soft copper matrix is helpful to lubrication, which causes the friction factor to reduce slightly compared with that of raw copper sample.

5. Conclusion

1. The surface composite layer of Cu-TiB_2 can be produced using the laser melting in situ synthesis. The size of TiB_2 particles is about 800 nm and the microhardness of composite layer can reach HV 210 when the volume fraction of TiB_2 increased to 20 vol.%, which is three times as large as that of raw copper.
2. The electrical conductivity is gradually reduced with increasing volume fraction of TiB_2 in the composite layer. However, the integrated conductivity of composite and copper substrate is reduced only marginally for sample, which can achieve more than 98% IACS at the volume fraction of TiB_2 of 20 vol.%.
3. The wear resistance of the laser melted in situ composite increases with increasing volume fraction of TiB_2. When the TiB_2 volume fraction is increased to 20 vol.%, the volume loss of composite is only 0.032 mm^3, and the wear resistance is 10 times better than the raw copper sample. The friction factors of all composite layer are concentrated around 0.115-0.13.

Acknowledgments

The work described in this paper was been financially supported by the Foundation of Natural Science of Department of Education, Shaanxi Province, China.

References

1. Z.Y. Ma, S.C. Tjong, and Z.Y. Ma, High Temperature Creep Behavior of In-situ TiB_2 Particlate Reinforced Copper-Based Composite, *Mater. Sci. Eng. A*, 2000, **284**, p 70
2. Y.G. Wang, Z. Zhang, G.H. Yan, and J.Th.M. De Hosson, Determination of Near Coincident Site Lattice Orientations in MgO/Cu Composite, *J. Mater. Sci.*, 2002, **37**, p 2511
3. E. Fras, A. Janas, A. Kolbus, and M. Gorny, Cu Plus TiC Composites Synthesis by RGI Process, *Arch. Metall.*, 1999, **44**, p 253
4. D.Y. Ying and D.L. Zhang, Processing of Cu-Al2O3 Metal Matrix Nanocomposite Materials by Using High Energy Ball Milling, *Mater. Sci. Eng. A*, 2000, **286**, p 152
5. J. Lee, N.J. Kim, J.Y. Jung, E.-S. Lee, and S. Ahn, The Influence of Reinforced Particle Fracture on Strengthening of Spray formed Cu-TiB_2 Composite, *Scripta Mater.*, 1998, **39**, p 1063
6. N. Zarrinfar, P.H. Shipway, A.R. Kennedy, and A. Saidi, Carbide Stoichiometry in TiC_x and Cu-TiC_x Produced by Self-Propagating High-Temperature Synthesis, *Scripta Mater.*, 2002, **46**, p 121
7. S.W. Russell, M.J. Rack, D. Adams, T.L. Alford, T.E. Levine, and M. Nastasi, Titanium Nitridation on Copper Surfaces, *J. Electro. Soc.*, 1996, **143**, p 2349
8. J.P. Tu, N.Y. Wang, and Y.Z. Yang, et al., Preparation and Properties of TiB_2 Nanoparticle Reinforced Copper Matrix Composites by In situ Processing, *Mater. Lett.*, 2002, **52**, p 448
9. K.L. Tee, L. Lu, and M.O. Lai, Synthesis of In situ Al-TiB_2 Composite Using Stir Cast Route, *Compos. Struct.*, 1999, **47**, p 589
10. S.C. Tjong and K.C. Lau, Abrasive Wear Behavior of TiB_2 Particle-Reinforced Copper Matrix Composite, *Mater. Sci. Eng. A*, 2000, **282**, p 183
11. V.V. Girzhon and T.A. Mal'Tseva, Structure State of Near-Surface Layers of a Steel 30 After Laser Assisted Alloying by Titanium Boride TiB_2, *Metallofizka I Noveishie TekhnologII*, 2005, **27**(10), p 1307–1316
12. J. Xu and W.J. Liu, Wear Characteristic of In situ Synthetic TiB_2 Particulate-Reinforced Al Matrix Composite Formed by Laser Cladding, *Wear*, 2006, **260**(4-5), p 486–492
13. J. Xu, W.J. Liu, Y.D. Kan, and M.L. Zhong, Microstructure and Wear Properties of Laser Cladding Ti-Al-Fe-B Coatings on AA2024 Aluminium Alloy, *Mater. Design*, 2006, **27**(5), p 405–410
14. J. Xu, Y.D. Kan, and W.J. Liu, In situ Synthetic TiB_2 Particulate Reinforced Metal Matrix Coating on AA2024 Aluminium Alloy Bu Laser Cladding Technology, *Surf. Rev. Lett.*, 2005, **12**(4), p 561–567
15. V. Ocelik, D. Matthews, and J.T.M. De Hosson, Sliding Wear Resistance of Metal Matrix Composite Layers Prepared by High Power Laser, *Surf. Coat. Technol.*, 2005, **197**(2-3), p 303–315
16. Q.W. Meng, L. Geng, and Z.H. Zheng. Laser Cladding Ni-Based Composite Coating on Titanium Alloy with Preplaced B4C+NiCoCrAlY, Pricm 5: The Fifth Pacific Rim International Conference on Advanced Materials and Processing, Pts 1-5 Materials Science Forum 475-479: 905–908, Part 1-5